


ORIGINAL ARTICLE

Neph2/Kirrel3 regulates sensory input, motor coordination, and home-cage activity in rodents

Linus A. Völker¹  | Barbara A. Maar¹ | Barbara A. Pulido Guevara¹ | Andras Bilkei-Gorzo² | Andreas Zimmer² | Hella Brönneke³ | Claudia Dafinger¹ | Sabine Bertsch¹ | Jan-Robin Wagener⁴ | Heiko Schweizer⁵ | Bernhard Schermer^{1,6,7} | Thomas Benzing^{1,6,7} | Martin Hoehne^{1,6,7}

¹Department II of Internal Medicine and Center for Molecular Medicine Cologne, University of Cologne, Cologne, Germany

²Institute of Molecular Psychiatry, Medical Faculty of the University of Bonn, Bonn, Germany

³Mouse Phenotyping Core Facility, Cologne Excellence Cluster on Cellular Stress Responses (CECAD), 50931 Cologne, Germany

⁴Institute for Neuroanatomy, Universitätsmedizin Göttingen, Georg-August-University Göttingen, Göttingen, Germany

⁵Renal Division, University Hospital Freiburg, Freiburg, Germany

⁶Cologne Excellence Cluster on Cellular Stress Responses in Aging-Associated Diseases (CECAD), University of Cologne, Cologne, Germany

⁷Systems Biology of Ageing Cologne (Sybacol), University of Cologne, Cologne, Germany

Correspondence

Linus Völker, Department II of Internal Medicine and Center for Molecular Medicine Cologne, University of Cologne, Kerpener Street 62, 50937 Cologne, Germany.
Email: linus.voelker@uk-koeln.de

Present address

Jan-Robin Wagener, Department of Basic Neurosciences, University of Geneva, Switzerland.
Heiko Schweizer, Helios Klinik Titisee-Neustadt, Department of Internal Medicine and Intensive Care Medicine, Titisee-Neustadt, Germany.

Adhesion molecules of the immunoglobulin superfamily (IgSF) are essential for neuronal synapse development across evolution and control various aspects of synapse formation and maturation. Neph2, also known as Kirrel3, is an IgSF adhesion molecule implicated in synapse formation, synaptic transmission and ultrastructure. In humans, defects in the NEPH2 gene have been associated with neurodevelopmental disorders such as Jacobsen syndrome, intellectual disability, and autism-spectrum disorders. However, the precise role in development and function of the nervous system is still unclear. Here, we present the histomorphological and phenotypical analysis of a constitutive *Neph2*-knockout mouse line. Knockout mice display defects in auditory sensory processing, motor skills, and hyperactivity in the home-cage analysis. Olfactory, memory and metabolic testing did not differ from controls. Despite the wide-spread expression of Neph2 in various brain areas, no gross anatomic defects could be observed. Neph2 protein could be located at the cerebellar pinceaux. It interacted with the pinceau core component neurofascin and other synaptic proteins thus suggesting a possible role in cerebellar synapse formation and circuit assembly. Our results suggest that Neph2/Kirrel3 acts on the synaptic ultrastructural level and neuronal wiring rather than on ontogenetic events affecting macroscopic structure. *Neph2*-knockout mice may provide a valuable rodent model for research on autism spectrum diseases and neurodevelopmental disorders.

KEYWORDS

attention-deficit hyperactivity disorder, autism-spectrum disorder, behavior, cerebellum, intellectual disability, Jacobsen syndrome, Kirrel3, knockout, Neph2, neurodevelopmental disorders, neurofascin, olfaction, phenotyping

1 | INTRODUCTION

Neph2 (or Kirrel3) is a cell-adhesion molecule of the immunoglobulin superfamily (IgSF). Members of this protein family carry extracellular immunoglobulin-like domains that mediate adhesion in a

calcium-independent manner. Neph2 consists of five such domains, a transmembrane domain, and a short cytoplasmic tail harboring a PDZ (Postsynaptic density 95, PSD-85; Discs large, Dlg; Zonula occludens-1, ZO-1)-binding motif at the C-terminus.¹ Neph2 is widely expressed during embryogenesis and adulthood.

Expression domains include the central nervous system, somites, branchial arches, extremity buds and the developing and adult sensory organs.^{2–6}

IgSF proteins have been shown to play a role in various organ systems and morphogenetic events. As a general principle, homophilic and heterophilic engagement of extracellular domains in *cis*- and *trans*-regulates cell adhesiveness, cell-cell recognition, and protein clustering at the plasma membrane. Signal transduction into the cell occurs via the intracellular tail (for review, see Refs. ^{7,8}). These proteins are conserved in evolution. In *Caenorhabditis elegans*, the Neph family protein SYG-1 has been shown to control synapse specificity and localization⁹ (cell). In the mouse olfactory bulb, Neph2 and its paralogue Neph3 modulate axonal guidance of olfactory sensory neurons (OSNs) into target glomeruli of the olfactory bulb. Neph2 and Neph3 are expressed in OSNs in an antidromic manner and thus help OSNs expressing the same olfactory receptor to converge on the same set of glomeruli.⁴ Differential expression of Neph proteins in subsets of OSNs leads to mistargeting. Neph2 appears to be required for proper morphogenesis of the accessory olfactory bulb and causes an increase in male-to-male aggression upon disruption.¹⁰ Inner and outer cochlear cells express Neph2 and are contacted by neuronal fibers that are immunoreactive for the IgSF-protein Nephrin.³ At the contact zone, a highly specialized synapse (ribbon synapse) is formed to ensure precise and ultrafast neurotransmitter release.¹¹

Martin et al recently described a role of Neph2 in hippocampal target-specific mossy fiber synapse development.¹² Moreover, recent evidence suggests an association of Neph2 with neurodevelopmental disorders and psychiatric diseases in humans: Genome-wide association studies report *NEPH2* as a candidate gene for autism spectrum as well as attention-deficit hyperactivity disorder (ADHD).^{13,14} In case reports, patients with partial deletions of the long arm of chromosome 11 (including the *NEPH2* locus) presented with intellectual disability and dysmorphic features consistent with Jacobsen syndrome.^{15–17}

In the present study, we aimed to elucidate the role of Neph2 in central nervous information processing. To this end, we generated a lacZ-knockin mouse strain of the *Neph2* locus by homologous recombination into embryonic stem cells. We used *in situ* hybridization (ISH) and immunofluorescence to identify neuronal circuits expressing Neph2 and performed according to the behavioral testing on knockin mice to clarify Neph2-function *in vivo*.

2 | METHODS

2.1 | Generation of lacZ-knockin (flox/flox) and full-body knockout (Δ/Δ) mice

A conditional knockin mouse line of the *Neph2* locus was generated by homologous recombination in 129 Sv/J (129S7/SvEvBrd) embryonic stem cells. Briefly, exon 2 of the endogenous *Neph2* locus was replaced by a cDNA consisting of exon 2–17 flanked by loxP sites that

was followed by an internal ribosomal entry site to enable expression of beta-galactosidase from the bacterial lacZ gene.¹⁸ Resulting chimaeras were tested for germline transmission, interbred with C57BL/6 mice and the positive selection neomycin/kanamycin cassette removed by mating with a flip-recombinase expressing mouse line. Resulting mice (Neph2^{flox/+}) were then bred to a Cytomegalovirus (CMV)-promoter driven cre-transgenic mouse line in C57BL/6 background to generate a constitutive knockout (Neph2 Δ/Δ , ie, Neph2^{flox/flox}; CMV.cre^{tg/+}).¹⁹ Some morphological experiments were conducted at this point of breeding. However, to rule out an influence of the CMV.cre-transgene on behavioral testing, we removed the CMV.cre allele from the mouse line by interbreeding heterozygous Neph2 Δ -mice that did not carry a CMV.cre allele (ie, Neph2 $\Delta/+$; CMV.cre^{+/+}). For experimental procedures, either Neph2 Δ/Δ -mice were bred to Neph2 $\Delta/+$ -mice to generate litters of 50% experimental (ie, Neph2 Δ/Δ) and 50% heterozygous control animals (ie, Neph2 $\Delta/+$) or alternatively, heterozygous mice (ie, Neph2 $\Delta/+$) were bred when it was reasonable to use Neph2 $\Delta/+$ -mice as additional controls. Male littermates were chosen exclusively for behavioral experiments to rule out strain and sex differences on behavioral traits. Mice were kept on a mixed background for all experiments. Throughout the manuscript, “+” indicates the wild-type allele and Δ indicates the knockout allele. Unless otherwise indicated, animals did not carry a CMV.cre-allele.

2.2 | Reverse-transcription polymerase chain reaction

The following primers were used on cDNA libraries generated from neocortex, olfactory bulb and cerebellum: Neph2—forward primer: 5'-GATGCTGTCTTCAGCTGTGCGT-3', reverse primer: 5'-CCCAGCATCCTCTTGCGGAC-3'; Hprt—forward primer: 5'-GCTGACCTGCTGGATTACAT and reverse primer 5'-TTGGGGCTGTACTGCTTAAC-3'.

2.3 | *In situ* hybridization

2.3.1 | Fixation and tissue processing

Animals were perfused transcardially with 15 mL of physiological saline, followed by 200 mL of 4% paraformaldehyde in 0.1 M phosphate buffer (PB), pH 7.4. The brains were dissected out of the skull and postfixed for 2 hours. Brains were then cryoprotected in 20% sucrose overnight at 4°C and sectioned either in coronal, or sagittal planes with a cryostat (Leica, Wetzlar, Germany) at 40 μ m thickness.

2.3.2 | *In situ* hybridization

ISH for Neph2 was performed with digoxigenin (DIG)-labeled cRNA probes. cRNA probes were generated from the appropriate plasmids containing full-length cDNA inserts of the respective gene (CloneID; Open Biosystems, Huntsville, Alabama): Neph2 5695003). After restriction digestions with appropriate enzymes and subsequent *in vitro* transcription using a DIG RNA labeling Kit (Roche, Basel, Switzerland), the size of the probes was reduced to 350 base pairs via alkaline hydrolysis (0.2 M sodium carbonate and 0.2 M sodium bicarbonate at pH 10.2).²⁰

The brain sections were rinsed thrice with 2X standard saline citrate (1x SSC = 0.15 M NaCl, 0.015 M sodium citrate, pH 7.0) and pre-treated for 15 minutes in hybridization buffer (HB; 50% formamide, 4x SSC, 250 µg/mL denaturated salmon sperm DNA, 100 µg/mL tRNA, 5% dextran sulfate and 1% Denhardt's solution) diluted 1:1 in 2x SSC at room temperature, followed by 1 hour in pure HB at 55°C. Probe hybridization with DIG-labeled probes (50 ng/mL) was done overnight at the same temperature. Post-hybridization washes were performed with 2x SSC (2x, 15 minutes, at room temperature), 2x SSC/50% formamide (15 minutes, at 65°C), 0.1x SSC/50% formamide (15 minutes, at 65°C), 0.1x SSC (2x, 15 minutes, at 65°C) and 0.01 M TBS, pH 7.5 (2 x 10 minutes, at room temperature). The probes were detected by anti-DIG Fab fragments conjugated to alkaline phosphatase (raised in sheep; Roche) diluted 1:1500 in TBS-containing blocking agent (at 4°C overnight). Hybridized probes were stained with nitro blue tetrazolium and 5-bromo-4-chloro-3-indolylphosphate (Roche). Development of the staining reaction was monitored with a binocular light microscope (Zeiss, Oberkochen, Germany). After the desired intensity was reached, the sections were rinsed again in TBS and mounted in Kaiser's glycerol gelatin (Merck, Darmstadt, Germany).

2.4 | Immunofluorescence

For immunofluorescence experiments, tissue was dehydrated in ascending ethanol concentrations and finally immersed in paraffin. Sections were cut to 4 to 8 µm thickness on a microtome and dried at 60°C for 6 hours. Slides were rehydrated in descending ethanol concentrations and washed in phosphate buffered solution. Antigen retrieval was performed at 120°C in Tris-EDTA pH 9.0 for 10 minutes (EDTA - Ethylenediaminetetraacetic acid). Blocking was done in 10% normalized donkey serum and 1% bovine serum albumin for 1 hour. The primary antibody was applied at 4°C overnight. The following primary antibodies were used: Polyclonal sheep biotinylated anti-Neph2 (R&D Systems, Minneapolis, MN; 1:100-1:200), polyclonal goat anti-Neph3 (R&D Systems; 1:500), polyclonal rabbit anti-MOR28 (MOR - mouse olfactory receptor; Osenses, Keswick, Australia; 1:1000), polyclonal rabbit anti-Calbindin (Abcam, Cambridge, UK; 1:200), polyclonal rabbit anti-HCN1 (Alomone Labs, Jerusalem, Israel; 1:200) and polyclonal rabbit anti-phosphorylated neurofilament heavy chain (pNF-h) (Covance, Princeton, New Jersey; 1:1000). Secondary antibodies were applied for 1 hour at reverse transcription. The following secondary antibodies were purchased from Jackson ImmunoResearch Laboratories, Inc. (West Grove, Pennsylvania) and used in a dilution of 1:1000: anti-sheep Cy3-conjugated, anti-rabbit DyLight488-conjugated, anti-rabbit DyLight649-conjugated and anti-goat DyLight549-conjugated. After washing, slides were embedded with ProLongGold and Hoechst with DAPI and visualized using a LSM 710/Axiobserver Z1 confocal microscope operated by ZEN 2009 software (all from Carl Zeiss Microimaging GmbH, Jena, Germany). The following objectives were used: x10/0.3, x20/0.8, x63/1.4 oil immersion objective (all from Carl Zeiss). Images were adjusted as to brightness and contrast. In cases of the biotinylated anti-Neph2 antibody, antibody detection was carried out using the TSA-amplification kit (PerkinElmer, Waltham, Massachusetts) and avidin/biotin blocking solutions (Vector Laboratories,

Burlingame, California) in some experiments. Alternatively, the Zenon-labeling kit (Molecular Probes, Eugene, Oregon) was used to visualize antibody binding according to the manufacturer's instructions for Zenon-555 and Zenon-647.

For serial sections of the olfactory bulb, tissue was embedded and staining was performed as described above. Sequential sections of the olfactory bulbs were cut at 4 µm thickness from posterior to anterior in a frontal plane, and four sections mounted per slide to provide an approximate estimate of the sections position within the olfactory bulb.

For bimolecular fluorescence complementation (BiFC), we generated full length as well as extracellular and intracellular truncations of Neph2 and neurofascin linked with either N-terminal or C-terminal part of the citrine fluorescent protein. Citrine, when reconstituted by close interaction of the N- and C-terminal-citrine fragment conjugated with candidate proteins, emits fluorescence. Specifically, the constructs comprised the following amino acid residues: Neph2 intracellular (ic) amino acid residues 535-777, Neph2 extracellular (ex) amino acid residues 22-556 and neurofascin extracellular (ex) amino acid residues 24-1238.

The following primers were used in cloning of the constructs:

1. Neph2 intracellular fp 5'-cgcgggacgcgtgtcatcatcggggtgg-3' rp 5'-ttgtatGCGGCCCGcGACGTGAGTCTGCATCCGCCG-3'
2. Neph2 extracellular fp 5'-cgc ggg acg cgt tac tcc ttc agc cag caa cc-3', rp 5'-ttgtatGCGGCCCGcCACAAATGGTTGCCATTAGGAC-3'
3. Neph2 full-length: fp 5'-cgc ggg acg cgt tac tcc ttc agc cag caa cc-3', rp 5'-ttgtatGCGGCCCGcGACGTGAGTCTGCATCCGCCG-3'
4. Neurofascin extracellular fp 5'-cgcgggacgcgtatcgaattctatggatc-caagc-3', rp 5'-cgcgggGCGGCCCGcGATGAAACAGACGATGAG-CAG-3'
5. Neurofascin full-length fp 5'-cgcgggacgcgtatcgaattctatggatc-caagc-3', rp 5'-cgcgggGCGGCCCGcggccagagagtagatagcatt-3'
6. Citrine-N-terminal fp: 5'-tata ggc ggc cgcgaggcagcgaggcgagg-gaagcGTGAGCAAGGGCGAGGAGCTG-3', rp: 5'-cgc ggg TCTAGA tta CTCGATGTTGTGGCGGATCTTGAAGTTCACC-3'
7. Citrine C-terminal fp 5'-tata ggc ggc cgcgaggcagcgaggcgagg-gaagcGACAAGCAGAAGAACGGCATC-3', rp 5'-cgc ggg TCTAGA tta CTTGTACAGCTCGTCCATGCCGAGAGTGATC-3'

HeLa (Henrietta Lacks) cells cultured under standard conditions (DMEM - Dulbecco's Modified Eagle's medium, 10% FCS, 5% CO₂, 37°C) were used for bimolecular fluorescence experiments and transfected using GeneJuice (Merck) according to the manufacturers' instructions.

2.5 | Plasmids and cloning

KCNA1-cDNA was a kind gift of René Bindels (Cambridge, UK). Kcna2-cDNA was a kind gift of Tony Morielli (Burlington, Vermont). NFASC (neurofascin) was amplified from IMAGE clone ID 9052980, accession number BC144454 (Open Biosystems, Thermo Scientific, Waltham, Massachusetts) using 5'-cgcgggacgcgtatcgaattctatggatc-caagc-3' (forward) and 5'-cgcgggcgccgcttagccagagtagatagc-3' (reverse) as primers. PSD-95 (discs, large homolog 4) was amplified

from a E10.5 mouse embryo cDNA library (ProQuest; Invitrogen, Carlsbad, California) using 5'-cgcgggacgcgtgccaccatggactgtctctgtagtg-3' (forward) and 5'-cgcgggcgccgctcagagtctctcgggctgg-3' (reverse) as primers.

2.6 | Cell culture, overexpression and coimmunoprecipitation

Cell culture, overexpression and coimmunoprecipitation were performed as previously described.²¹ In brief, HEK293T cells were grown to 60% to 80% confluency under standard conditions (DMEM, 10% FCS, 5% CO₂, 37°C), were transfected using the calcium-phosphate method. After incubation for 24 hours, the cells were lysed in ice-cold modified radioimmune precipitation assay buffer (50 mM Tris [pH 7.5], 150 mM NaCl, 1% Nonidet P-40, 0.25% sodium deoxycholate, 1 mM NaF, 1 mM EDTA, 0.25 mM PMSF and 5 mM Na₃VO₄) and cleared by ultracentrifugation (Beckmann TLA-55, 50 000 rpm, 4°C, 60 minutes). Equal measures of protein in the supernatant were incubated for 1.5 hours at 4°C with anti-FLAG M2-agarose beads (Sigma-Aldrich, St. Louis, Missouri). After extensive washing, bound proteins were resolved by 10% sodium dodecyl sulfate-polyacrylamide gel electrophoresis.

2.7 | Animals

For behavioral testings, age-matched male littermates between 9 and 20 weeks were used. All animal testing was done in accordance with the rules and regulations of the institutions of the University of Cologne and the University of Bonn. Animals were allowed to accustom to the new environment and entrain to the inverted light cycle for 2 weeks before any behavioral testing. The animals were left undisturbed for 6 to 7 days between the tests. Order and number of tests per animal were equal among control and experimental animals and conducted in groups consisting of experimental and control animals. Experiments were conducted during the dark phase of the inverted 12 hours dark/12 hour light cycle under red-light conditions. Test order was: Open Field - Odor Discrimination - Startle Response for all animals. Half of the cohort continued to Rotarod testing while the other half was assessed in the home-cage setting. A separate group of mice underwent the Startle Response and the Novel Object Recognition test.

2.8 | General health assessment

Neph2^{Δ/Δ} and Neph2^{Δ/+} mice (16 per genotype) were subjected to a general health assessment to rule out gross anatomic or sensory defects that could potentially interfere with behavioral testing and would result in false positives. The tests were carried out as laid out previously.^{22–25} Percentage of mice displaying the indicated behavior is shown. In some instances, a 3-point rating scale was used at the discretion of the observer.

2.9 | Home-cage activity

Animals were placed into individual cages, received food and water ad libitum, and left undisturbed for 6 days. The motor activity of the mice

was measured using the automatic Mouse-E-Motion system (Infra-E-Motion GmbH, Hamburg, Germany). The motor activity values were registered in every 30th minute and compared between the groups using two-way ANOVA (between factor: genotype, within factor: time). Recordings were obtained during a time span of 48 hours and averaged per time point.

2.10 | Open-field test

Motor activity was measured in a 42 × 42 × 25 cm arena for 30 minutes as interruptions of infrared beams using the ActiMot system (TSE Systems GmbH, Bad Homburg, Germany). The test was carried out in a sound and light isolated environment under dim light (light intensity at the floor level was 15 lx). Dim light conditions had been shown not to be different from red-light conditions by the authors in preliminary studies. Distance traveled, number of rears and time spent in the central part of the arena were registered in every fifth minute and analyzed using two-way ANOVA (between factor: genotype, within factor: time).

2.11 | Odor test

The animals were habituated to the test environment placing them into an open-field arena for 5 minutes in three consecutive days. At day 4, three 3 × 3 cm filter paper was fixed onto the floor: one was made wet with water, the second with 0.1% cinnamon solution (which was shown as a neutral stimulus in previous studies by the authors), the third with urine of a female mouse. Time spent with investigating the filter papers was measured for 5 minutes using The Observer XT System (Noldus, Wageningen, The Netherlands). Groups were compared using two-way ANOVA (between factors: genotype and odor).

2.12 | Startle test

To test the hearing ability, we used the startle test. The animals were placed in a small cage on a vibration sensitive platform in a sound isolated chamber equipped with two speakers. Then, 65-dB background noise was present during the whole experiment in the chamber. In the first phase of the test after 5 minutes habituation, two 100 ms 110 dB 12 kHz sound were presented. The reactivity of the animals to randomly presented sound stimuli (four times 100 ms 12 kHz sound with 80, 90, 100 or 110 dB intensity) was registered in the next phase. The mean startle reactivity to the four stimuli was calculated and used for the statistical analysis. Groups were compared using two-way ANOVA (between factors: genotype and sound intensity).

2.13 | Rotarod test

To determine the locomotion and coordination of the mice, we used the Rotarod test. The animals were placed on a rotating rod (2–40 rpm with an acceleration of 2.5 rpm/s; Ugo-Basile, Gemonio, VA, Italy) and the falling times were determined. Each animal had 10 trials. We calculated the mean of the time the mice spent on the rod for each trial. Groups were compared using repeated measures ANOVA (categorical factor: genotype, within effect: time) and Bonferroni's multiple comparisons test applied to compare time points.

2.14 | Object recognition test

Object recognition test was conducted as previously described.²⁶

2.15 | Indirect calorimetry, activity, food and water sensors

Automatic recording and analyzing of metabolic parameters as energy expenditure and respiratory exchange ratio were performed in an indirect open-circuit calorimetry system (PhenoMaster System; TSE Systems). Food and water intake were determined simultaneously to the indirect calorimetry measurements with build-in automated scales. Mice were kept at 22°C to 24°C and were allowed to acclimatize in the chambers (Type II cages, 7.1 L) for at least 24 hours. Food and water were provided ad libitum in the appropriate devices. Data were collected for at least 48 hours. Unpaired student's *t* test was used to calculate significance for difference. Groups were compared using two-way ANOVA (genotype, time) followed by Bonferroni's multiple comparisons test to compare time points.

3 | RESULTS

3.1 | Confirmation of *Neph2*-full-body knockout mice

To better understand the role of *Neph2* controlled synapse specificity in controlling behavior of the organism, we generated mice where the *Neph2* gene was flanked by loxP sites¹⁸ and mated these *Neph2*^{fllox/fllox} mice with mice that express Cre recombinase under the control of the ubiquitously expressing CMV promoter. In homozygous knockout mice, neither *Neph2* mRNA nor protein expression could be detected in any tissue examined confirming the *Neph2* gene deletion (Figure 1). Knockout mice did not display any gross anatomic phenotype (data not shown) or abnormalities in a general health assessment (Table S1, Supporting Information). Before starting the behavioral experiments, we analyzed the expression pattern of *Neph2* in the mouse brain in adult animals by ISH. Among other tissues, *Neph2* mRNA showed a distinct expression pattern. *Neph2* is specifically expressed in periglomerular and mitral cells of the olfactory bulb, layer 2/3- and layer 5-specific cells throughout the neocortex, and molecular layer interneurons of the cerebellum (Figure 2). Expression in the otic vesicle, cochlear hair cells and the hippocampus had been shown before.^{3,6}

3.2 | *Neph2* in auditory sensory processing

Next, we performed behavioral testing on age-matched male littermates. Specifically, the expression in inner and outer cochlear hair cells prompted us to test auditory perception in *Neph2*^{Δ/Δ}-mice in the acoustic startle setup. Mice were placed on a vibration sensitive platform and exposed to 65-dB background noise. Mice were then subjected to auditory stimuli of increasing intensity in the acoustic startle test. Intensities ranged from 80 to 110 dB in 10 dB increments and were presented four times with a duration of 100 ms. The reaction intensity was measured by the degree of excursion of the platform in response to the startle reaction of the animal. Interestingly, the

response of *Neph2*^{Δ/Δ}-mice to stimuli of 110 dB was significantly diminished in comparison to *Neph2*^{Δ/+}-mice ($P < 0.01$, as calculated by two-way ANOVA; effect of genotype in two-way ANOVA $F_{(1,104)} = 12.22$, $P = 0.0007$. There was no relevant interaction: $F_{(3,104)} = 1.577$, $P = 0.1995$). A trend toward a less intensive reaction could already be noted at sound intensities of 80, 90 and 100 dB but did not reach statistical significance. Initial experiments were performed at 10 to 20 weeks on $N = 13$ and $N = 15$ mice, respectively. To rule out selection bias in the test groups due to the well-documented presbycusis phenotype in C57/B6 mouse strains, we repeated the experiments with mice at 9 weeks of age.²⁷ Results confirmed our previous findings and ruled out an age-related bias.

3.3 | *Neph2* in olfactory sensory processing

Neph2 and other cell-adhesion molecules have been implicated in axonal targeting of OSNs to glomeruli of the olfactory bulb. Expression levels of cell-adhesion molecules form a specific cell-surface pattern that is used as a code to bundle and converge OSNs expressing the same cell-surface marker set.⁴ To test whether the deletion of *Neph2* from OSNs leads to aberrant axonal targeting, we stained serial sections of wild-type and knockout olfactory bulbs for MOR28 (mouse olfactory receptor 28). MOR28 expression had previously been strongly correlated with high *Neph2* levels in OSNs.⁴ However, in *Neph2*^{Δ/Δ}-mice, number and topographical position of MOR28-positive glomeruli in the OB did not appear to be different from wild-type mice. Moreover, expression levels of *Neph3* in the glomerular layer did not change upon loss of *Neph2* (Figure 4) suggesting the absence of profound disturbances of the neuronal identity code. In an olfactory test setup utilizing two different odor samples, the general ability of knockout animals to discriminate odors did not appear to be altered (Figure 3B). Experimental animals displayed the same typical increased interest in social odors (urine) as compared with nonsocial neutral odors (cinnamon) suggesting an intact olfactory sensory processing on higher brain levels.

3.4 | *Neph2* in motor coordination

IgSF proteins including *Neph2* have been implicated in motor-associated organ systems and neuronal circuits. Expression in the cerebellar cortex, pontine nuclei, dorsal root ganglia and dorsal somites has been described previously.^{5,28} By immunofluorescence, we could detect *Neph2* protein in the cerebellum at the pinceau of Purkinje cells as determined by the coexpression of HCN1 (hyperpolarity cyclic nucleotide gated channel 1), a well-established pinceau marker²⁹ (Figure 5A,B). At this highly specialized structure, basket cell collaterals form GABAergic form synapses onto Purkinje cell bodies and axon initial segments. Thus, we hypothesized a role of *Neph2* in motor abilities and coordination. To test for a role of *Neph2* in pinceau formation, we used the pinceau marker HCN1 to assess pinceau morphology in *Neph2*^{Δ/Δ}-mice and pNF-H to visualize basket cell axon projections onto Purkinje cells. *Neph2* is expressed consistently across all cerebellar columns at the pinceau (Figure 5A), and the anatomical structure of the pinceau is preserved in *Neph2*^{Δ/Δ}-mice (Figure 5B). Basket cell projections were oriented perpendicular to the Purkinje

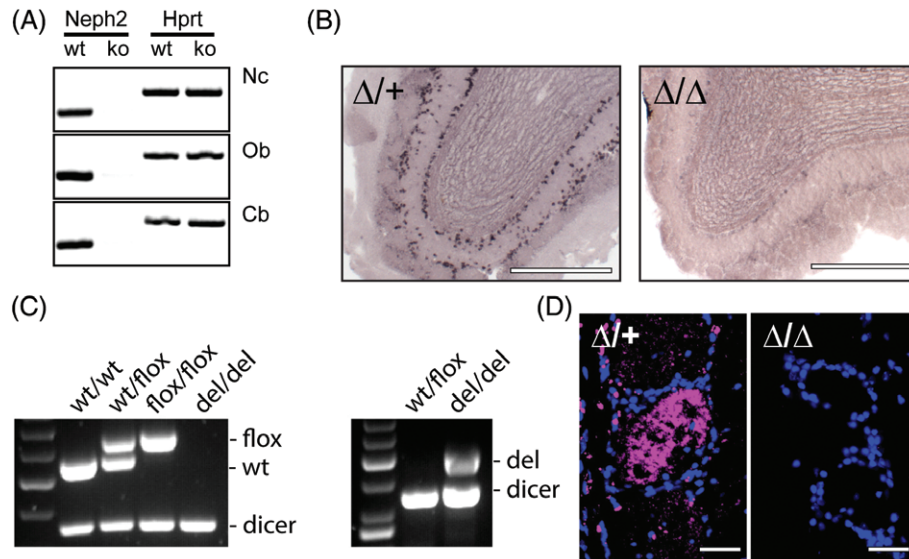


FIGURE 1 Proof of knockout—(A) RT-PCR of *Neph2* on mRNA isolated from different neuronal tissues (Nc, neocortex; Ob, olfactory bulb; Cb, cerebellum) from wild type (wt) and *Neph2*^{Δ/Δ}-mice (ko). (B) ISH of *Neph2*-transcripts on *Neph2*^{Δ/+}; CMV.cre^{tg/+} and *Neph2*^{Δ/Δ}; CMV.cre^{tg/+} knockout tissue shows *Neph2* mRNA to be absent from *Neph2*^{Δ/Δ} knockout tissue. Scale bars represent 500 μm. (C) PCR products used in genotyping of *Neph2*^{Δ/Δ}-mice. In a first PCR, primers were used to detect the wild-type and floxed alleles of the *Neph2* locus. A PCR for dicer was run as endogenous control because tissue from full-body-knockout mice did not yield any wild-type- or flox-specific PCR product. In a second PCR, the presence of a compacted deletion-allele after cre-exposure was determined. (D) Lack of *Neph2*-protein could also be shown by immunofluorescence on tissue section of olfactory bulbs. This area typically exhibits strong Neph-protein expression. *Neph2* immunofluorescence is shown in magenta, DAPI in blue. Scale bars represent 50 μm

cell layer and engulfed Purkinje cell bodies in the eponymous basket-like manner (Figure 5B).

Next, we performed the Rotarod test to evaluate motor coordination, balance and motor learning in vivo. *Neph2*^{Δ/Δ}-mice perform slightly better in the Rotarod test but only two trials (#2 and #4) reached statistical significance (Figure 3C, repeated measure ANOVA followed by Bonferroni's multiple comparisons test * $P < 0.5$, *** $P < 0.001$; two-way ANOVA reported $F_{(1,130)} = 52.95$, $P < 0.0001$ for "genotype"). Concordantly, general motor activity as measured by the total distance traveled in the open-field test as well as gait and posture did not differ in *Neph2*^{Δ/+} and *Neph2*^{Δ/Δ}-mice (Figure 3E;

Table S1). We then focused on the putative role of *Neph2* on synapse assembly and function by screening for interactions between *Neph2* and proteins of the synaptic scaffold or the cerebellar pinceau in particular.^{30,31} An interaction with the synaptic protein CASK had been shown before.² In overexpression experiments in HEK293T cells, *Neph2* interacted with synapse-associated proteins such as PSD95 as well as pinceau-associated ion-channels Kv1.1, Kv1.2 and the cell adhesion molecule neurofascin (Figure 6). By BiFC, we could show a close interaction of the extracellular domains of *Neph2* and neurofascin indicating modulation of cell-cell-adhesion putatively via Ig-domains (Figure 7). Well-documented homophilic interactions of

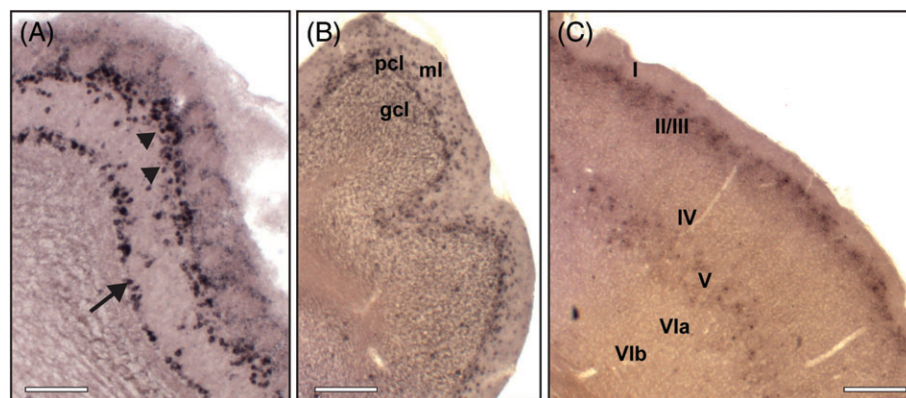


FIGURE 2 *Neph2* expression analysis—ISH of *Neph2* mRNA on wild-type adult tissue. Expression of *Neph2* could be detected in the olfactory bulb in the mitral cell layer (A; arrow) and the periglomerular cells of olfactory glomeruli (A; arrow heads). In the cerebellum, we found *Neph2* mRNA predominantly expressed in the inner third of the molecular layer (B; ml). In a frontal section of the neocortex, *Neph2* was expressed by cells in layer II/III and V (C). Scale bars represent 200 μm

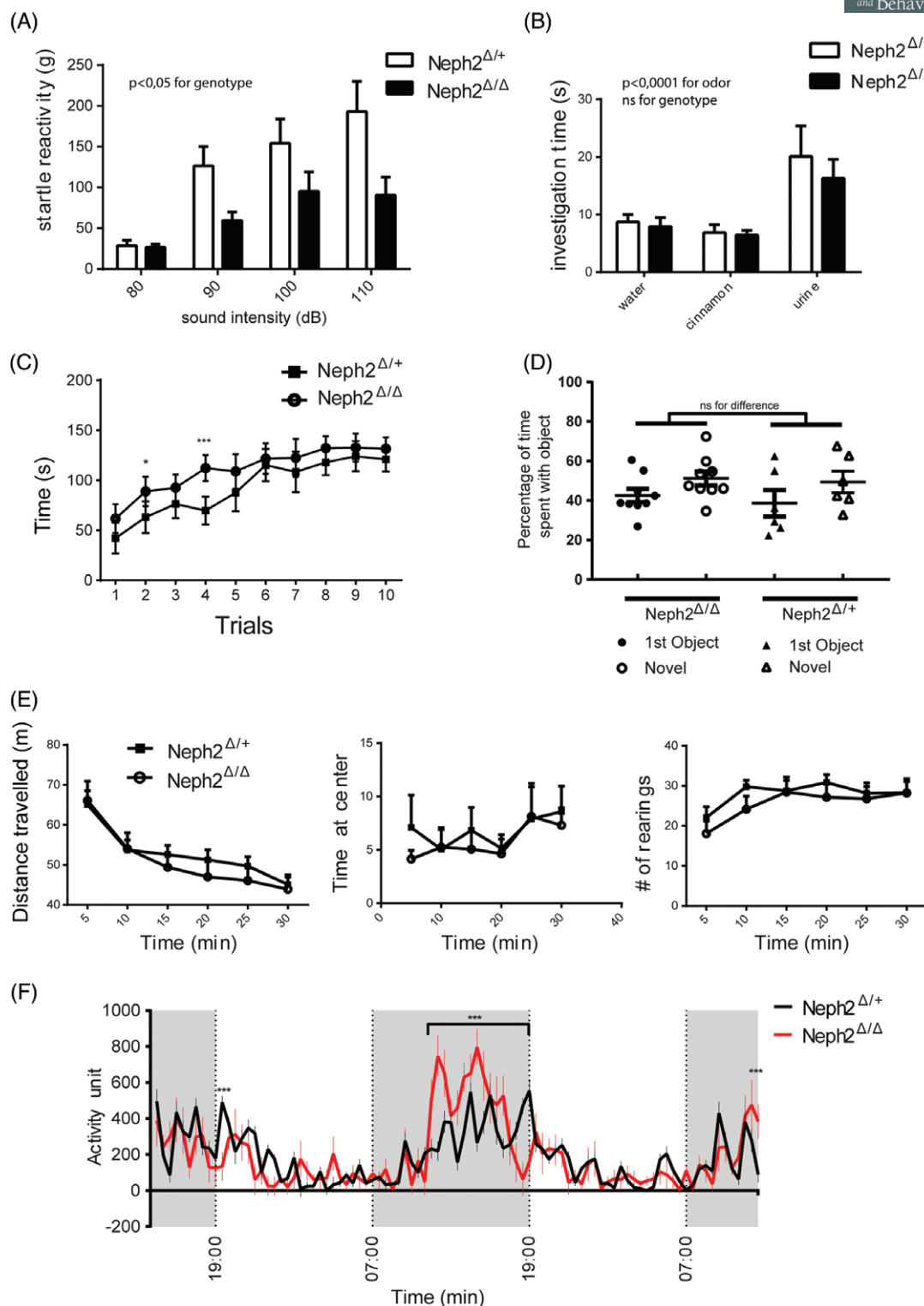


FIGURE 3 Behavioral phenotyping—(A) *Neph2*^{Δ/Δ}-mice displayed a significantly reduced reaction to acoustic stimuli as tested in the startle response setting. This became evident particularly at higher sound intensities (*Neph2*^{Δ/Δ} $N = 13$, *Neph2*^{Δ/+} $N = 15$). Two-way ANOVA $** P < 0.05$. (B) The odor discrimination test confirmed an intact sense of smell as mice could equally distinguish between different odors. A neutral cotton swab was presented in parallel to rule out novelty-induced investigation as a confounding variable (*Neph2*^{Δ/Δ} $N = 15$, *Neph2*^{Δ/+} $N = 14$; two-way ANOVA $**** P > 0.0001$ for odor as source of variation, no interaction $F_{(2,54)} = 0.2835$, $P = 0.7542$). (C) Control and *Neph2*^{Δ/Δ}-mice performed marginally better in the RotaRod test. However, only two trials (#2 and #4) reached statistical significance. (*Neph2*^{Δ/Δ} $N = 8$, *Neph2*^{Δ/+} $N = 7$). Repeated measure ANOVA $* P < 0.5$, $*** P < 0.001$. (D) Novel object recognition test was performed to test for recognition memory. There were no notable differences between genotypes indicating an unimpaired recognition memory in *Neph2*^{Δ/Δ}-mice (*Neph2*^{Δ/Δ} $N = 9$, *Neph2*^{Δ/+} $N = 5$). Unpaired student's t test for difference; repeated measure ANOVA indicated the presentation of a novel object as a significant source of variation ($* P < 0.05$). Genotype was no significant source of variation ($P = 0.58$). (E) No differences between genotypes were observed in the open field test. Equal measurements of the distance traveled in a particular time interval and equal number of rearings indicate similar territorial exploratory behavior. Time at center was recorded as a measurement of fear and anxiety in novel surroundings (*Neph2*^{Δ/Δ} $N = 13$, *Neph2*^{Δ/+} $N = 14$). (F) Activity patterns of control and *Neph2*^{Δ/Δ}-mice were recorded using the mouse-E-motion system while mice were on an inverted 12 hours light/12 hours dark cycle. *Neph2*^{Δ/Δ}-mice displayed bursts of activity on repeated measurements during the dark phase. (*Neph2*^{Δ/Δ} $N = 8$, *Neph2*^{Δ/+} $N = 6$). Two-way ANOVA followed by Bonferroni's multiple comparisons test to compare time points, $*** P < 0.001$.

extracellular domains of Neph2 in *cis* were used as a positive control.

3.5 | Neph2 in higher brain functions

There has been an increasing body of evidence supporting a role of Neph2 in neurodevelopmental disorders such as ADHD, autism, intellectual disability and Jacobsen syndrome.^{16,32} In mice, *Neph2* mRNA is expressed in various telencephalic and mesencephalic structures such as the neocortex, the thalamus, the hypothalamus and the hippocampus (Figure 2; Ref. ⁶). Precisely, we could localize *Neph2* expression in the neocortex to cortical layers 2/3 and 5. Albeit being indicative of neuronal expression, we cannot rule out that other cell types are the source of *Neph2* positivity. Evidence has accumulated that Neph2 plays a role in synapse specification. Moreover, most of proteins encoded by genes related to autism-spectrum disorders (ASDs) are involved in synapse formation. Because disturbances of higher brain functions represent a key feature of ASD and are too complex to be sufficiently accessible through neuroanatomic and morphologic

analysis, we addressed a putative function of Neph2 in brain functions such as fear/anxiety, memory, feeding behavior as well as day-night activity pattern by behavioral testing. To this end, we performed open-field and object recognition tests as well as home-cage and empty-cage activity, and PhenoMaster analysis of food and water intake and energy expenditure. As a classic prey animal in predation, mice tend to avoid open, well-lit areas and mostly confine themselves to the cage walls. The object recognition test is a simple study of memory as well as exploratory behavior/interest in novel objects. Home-cage and empty-cage tests provide an insight into exploratory behavior in unknown and known environments, activity levels and social interactions with cage mates. Ultimately, the PhenoMaster test measures time and amount of food and water consumption as well as overall energy expenditure as a measurement of general activity levels or metabolic changes.

Control and knockout mice spent equal amounts of time investigating a known object in the object-recognition test. There was no difference in the amount of additional time both groups spent investigating a novel object indicating no differences in memory function or novelty induced behavior (Figure 3D). The novel object was reliably recognized by both animal cohorts. Exploratory behavior as a surrogate for anxiety and general activity levels in the open-field test was not significantly different in both groups (Figure 3E).

While there was no significant difference in anxiety, memory, novelty induced behavior, or feeding associated behaviors (Table S1 and Figure S1), *Neph2*^{Δ/Δ}-mice shown burst-like phases of hyperactivity during parts of the dark cycle (Figure 3F, repeated measures two-way ANOVA followed by Bonferroni's multiple comparisons test for timepoints, ****P* < 0.001, two-way ANOVA reports *F*_(6,120), *P* < 0.0001 for genotype as source of variation). These data suggest that Neph2 causes hyperactivity and disturbances of the day-night cycle that resemble behaviors observed in individuals with ASD. Our findings contribute additional information on the phenotype of Neph2-deficient mice and underscore the necessity to conduct behavioral tests in addition to morphologic and biochemical studies to fully grasp the role of cell-adhesion molecules of the Neph family in synapse formation and regulation of higher brain functions.

4 | DISCUSSION

In the present study, we provide an analysis of the behavioral and anatomical phenotype of *Neph2*^{Δ/Δ}-mice. We show that in contrast to the wide-spread expression of Neph2 in development and our expectations based therein, *Neph2*^{Δ/Δ}-mice display only minor phenotypical abnormalities. These include sensory deficits and changes in activity and motor coordination. We could not detect phenotypical alterations or gross anatomical deficits in the additional Neph2-expressing circuits examined.

In humans, the *NEPH2* gene has recently been implicated in neurodevelopmental disorders and psychiatric disease such as Jacobsen syndrome, intellectual disability, autism and ADHD. This lead us to surmise that Neph2 preferably acts on neuronal circuit assembly at the synapse level because many neurodevelopmental and ASD-related proteins act on synapse formation and plasticity. Defects in

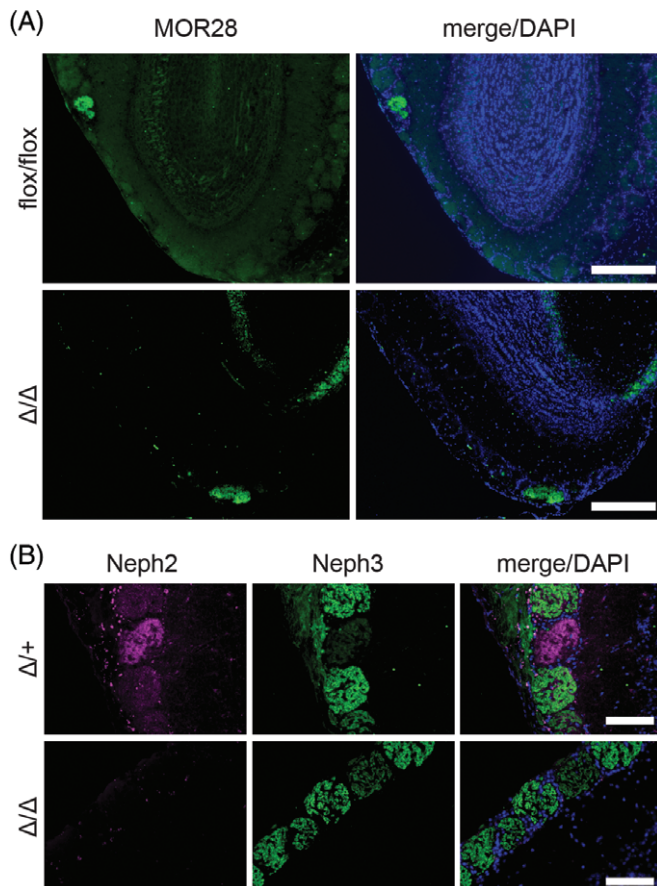


FIGURE 4 Morphological analysis of the olfactory bulb— (A) Immunofluorescent stainings of representative section of the olfactory bulb of control (*Neph2*^{flox/flox}; CMV.cre^{+/+}) and experimental animals (*Neph2*^{Δ/Δ}; CMV.cre^{+/+}). MOR28 labeled in green as indicated. Position and number of MOR28-positive olfactory glomeruli did not differ in control and Neph2-knockout mice. Scale bars represent 400 μm. (B) Also, overall levels and distribution of the reciprocally expressed Neph3 was unaffected by Neph2-knockout (upper row *Neph2*^{Δ/+}, lower row *Neph2*^{Δ/Δ}). Scale bars represent 100 μm

fine-tuning synaptic plasticity, synapse formation and connectivity patterns might stand out more prominently in complex neuronal traits such as activity levels, circadian rhythm/sleep regulation, social behaviors, memory and sensory input processing. In consideration of recent associations of *Neph2* in CNS-related disorders, we find it promising to expand on the idea of the *Neph2* knockout mouse as a putative model for ASD/neurodevelopmental disorders by exploring typical traits such as repetitive behavior, social interaction, attention deficit and sleep disturbances by appropriate experimental tests in future studies.

Interestingly, *Neph2*-full body knockout mouse lines that display some similar and some conflicting phenotypical data have recently been reported.^{33,34} It is imaginable that discrepancies are

caused by difference in genetic engineering or the genetic background of the lines. Behavioral experiments greatly depend on environmental factors, and minor changes in the experimental setting such as the order of tests or time of the day when experiments are conducted might alter the results or hamper the detection of subtle phenotypes. Moreover, while Hisaoka and colleagues used wild-type mice as controls, we used heterozygous *Neph2*-knockout mice thus possibly attenuating phenotypical differences. Yet, all three studies emphasize the role of *Neph2* in controlling neuronal function via synapse formation and plasticity and prompt to interpret behavioral experiments with diligence and regards to confounding variables.

Data from invertebrates and recent data on mammals provide strong support for the notion that *Neph2* is involved in

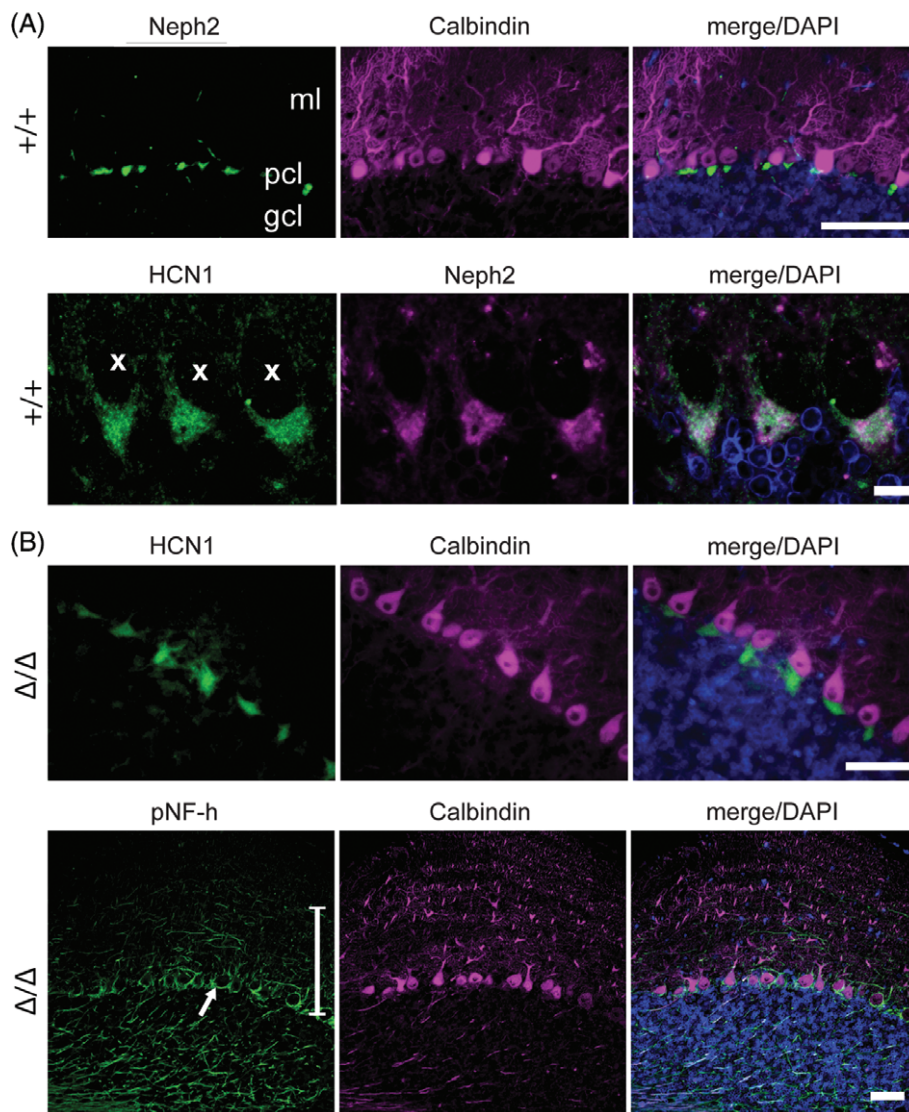


FIGURE 5 *Neph2* in the cerebellum—(A) Analysis of *Neph2* expression in C57BL/6 wild-type mice (purchased from Charles River). *Neph2* expression could be localized to the cerebellar pinceau, a dense array of axo-axonal synapses at the axon initial segment of cerebellar Purkinje cells. Cerebellar layers are labeled as molecular layer (ml), Purkinje cell layer (pcl) and granule cell layer (gcl). Purkinje cells have been immunofluorescently labeled with calbindin. *Neph2* colocalizes with the pinceau-marker HCN1. Purkinje cell bodies are marked by an X for orientation. (B) Analysis of cerebellar anatomy in *Neph2*^{Δ/Δ}-mice. The cerebellar pinceau correctly forms in *Neph2*^{Δ/Δ}-mice as shown by typical HCN1 staining. Basket cell axons and their collaterals have been labeled with and antibody directed against pNF-h to study basket cell projections onto Purkinje cells. Basket cells are mainly localized in the inner third of the molecular layer (as indicated by white lines) and form eponymous axon terminals around the cell bodies and axon initial segment of Purkinje cells (white arrows). These projections correctly form in *Neph2*^{Δ/Δ}-mice. Scale bars represent 100 μ m in (A - upper panel), 10 μ m in (A- lower panel) and 50 μ m in (B)

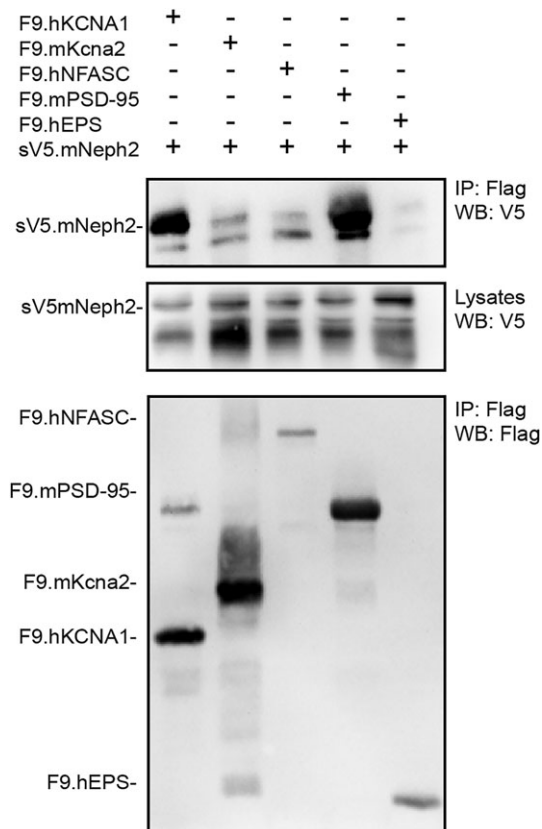


FIGURE 6 Neph2 interacts with synaptic proteins—in overexpression experiments in HEK293T cells, we could prove an interaction of Neph2 with proteins known to be localized at the cerebellar pinceau (Kv1.1, Kv1.2, neurofascin). In addition, Neph2 interacted with the ubiquitous synaptic scaffold PSD95, putatively via its PDZ-binding domain. FLAG-tagged synaptic proteins (KCNA1, Kcna2, NFASC, PSD-95) or control protein (EPS) were precipitated and precipitates were analyzed for co-precipitating V5-tagged Neph2

spatiotemporal synapse formation, synaptic transmission levels, and synaptic ultrastructure, particularly in the hippocampus.^{12,35–37} It is tempting to surmise that Neph2 exerts similar effects on synapses in the auditory, cerebellar and olfactory circuits. Ultrastructural and electrophysiological approaches are warranted.

As suggested by our data, Neph2 most likely acts on multiple levels of neuronal circuit assembly depending on the organ system or morphogenetic event in question. Neph2 has been associated with synaptogenesis, synaptic plasticity, axonal pathfinding, target cell recognition, and cell migration.^{4,9,38,39} The phenotypical outcome in a particular organ system or circuitry may greatly depend on the presence of redundant adhesion molecules (such as other IgSF proteins) or the quantity and quality of Neph2-protein action on a particular molecular mechanism.

All experiments in this study have been conducted on whole-body knockout mice. However, in some organ system (eg, the olfactory bulb or possibly the cerebellum), not absolute expression levels but levels relative to other neuronal subpopulations seem to bring about a specific phenotype. Sakano and colleagues could show that the overexpression of Neph2 in a subset of OSNs led to aberrant axonal targeting.⁴

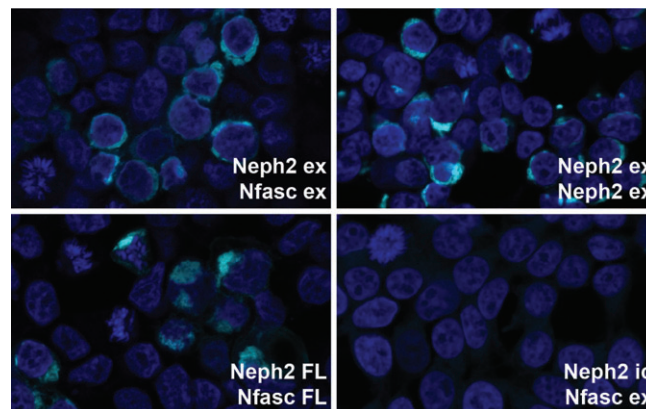


FIGURE 7 Interaction of the extracellular domains of Neph2 and neurofascin—we used BiFC of citrine to show interactions of the extracellular domains of Neph2 and neurofascin. Truncated or full-length variants of Neph2 and/or neurofascin fused to an N- or C-terminal citrine truncation were transfected into HeLa cells. Fluorescence can only be visualized when the N-terminal citrine truncation is complemented by its C-terminal counterpart indicating a close spatial proximity of both carrier molecules. As expected, interaction and complementation of citrine took place when full-length protein of Neph2 and neurofascin as well as only the extracellular and transmembrane domains were used. Interaction of citrine fragments by chance is ruled out by the negative control of noninteracting fusion partners Neph2-intracellular domain (Neph2 ic) and neurofascin-extracellular (+transmembrane) domain (Nfasc ex)

To test whether the knockout of Neph2 in the olfactory bulb causes aberrant axonal targeting, the differential knockout in a specific subset of OSNs by MOR-driven cre-lines appears a promising approach. Furthermore, generating double or even triple knockout mouse lines of Neph2 and additional members of the IgSF may yield more detailed information on the interplay of cell adhesion molecules in the composition of the neuronal identity code of the olfactory bulb.

Neph2 is expressed in inner and outer cochlear hair cells providing a correlate for hearing disabilities as observed in the acoustic startle response test in Neph2^{Δ/Δ}-mice. It is intriguing to speculate that ribbon synapse formation on inner hair cells as an important hub for auditory information processing may depend on Neph2-protein action. More extensive testing including evoked auditory brain stem potentials, otoacoustic emissions and immunofluorescent and electron microscopic histological analysis of the inner ear will eventually help specify the site of abnormal signal processing in the auditory system. To fully clarify whether the observed phenotype represents a hearing deficit or rather an impaired startle response, the startle response may be elicited by a tactile stimulus such as an air puff.

Novel object recognition was not impaired in Neph2^{Δ/Δ} mice contrary to findings by others.³³ As the effect size appears to be small, the animal numbers in this study might have been underpowered to detect subtle differences.

The differences in diurnal activity levels in home-cage analysis may have resulted from different causes: While it cannot be ruled out that there are differences in circadian rhythm, more sophisticated experimental setups are needed to confirm this. For example, mice could be held in permanent darkness to observe activity levels

without relation to the light phases. Alternatively, mutant mice may have reacted earlier and more intensively to the start of the dark phase, and extending the experiment over the course of several days may help exclude external environmental factors triggering the spike in activity. However, despite some uncertainty, results by others also indicate increased home-cage activity.³³ While we did not observe any measurable differences in the open-field test under red light or dim light conditions in preliminary experiments, an influence of the lighting on mice with a putatively disturbed circadian rhythm may yield different results and needs to be addressed in future experiments.

Data from ISH experiments, expression arrays and a study from Nishida and colleagues suggested a role for Neph2 in neuronal motor circuits.^{5,28,39,40} By immunofluorescence, we could localize Neph2-protein expression to the cerebellar pinceau in line with the expression in molecular layer interneurons as reported by Paul and colleagues. The linear anatomy of the cerebellar circuitry and the well-defined expression domain of Neph2 at the cerebellar pinceau provided an excellent model system to scrutinize Neph2 function on molecular level. Neph2 interacts with ion channels of the pinceau and with a central organizer of the pinceau, the cell adhesion molecule neurofascin. We hypothesized that Neph2 is involved in either axonal guidance of basket cell axons to Purkinje cells on global or subcellular level, in pinceau formation, or in regulating the conductive properties of synaptic connections between basket cell axons and the axon initial segment of Purkinje cells. Yet, a global staining of basket cell axons by pNF-h provided no indication of guidance defects. Dye filling experiments of single basket cells may conclusively address this question. Electrophysiological patch clamp experiments to measure Purkinje cell output might shed light on the effect of Neph2 on basket cell inhibitory activity and synapse formation at the pinceau.

As assessed by immunofluorescence, the anatomy of the cerebellar pinceau was preserved in Neph2^{Δ/Δ}-mice. Based on studies of knockouts of pinceau-localized proteins, it has become evident that the structural integrity of the cerebellar pinceau is mainly dependent on the interaction of AnkryinG and neurofascin while knockouts of other pinceau-localized adhesion molecules such as L1, NrCAM and CHL1 did not affect pinceau anatomy.⁴¹ Possibly, the module of AnkryinG and neurofascin clusters cell adhesion molecules at the pinceau to construct a neuronal identity code that helps axons of local basket cells expressing a complementary set of adhesion molecules including Neph2 to home in on target Purkinje cells. Neph2^{Δ/Δ}-mice appeared to perform marginally better in the rotarod test but only two trials (#2 and #4) reached statistical significance. Similar experiments in a recently published paper involving a different full-body Neph2-knockout mouse line clearly shown an improved motor coordination over control mice³⁴ leading us to believe that the observed trend represents a true phenotype rather than coincidence. If the hypothesis holds true that the cerebellar circuitry depends on neuronal identity codes and relative expression levels as seen in the olfactory system, a subgroup-specific knockout may help clarify the role of Neph2 herein.^{42,43}

Conflict of interest

The authors claim no conflict of interests.

ORCID

Linus A. Völker  <https://orcid.org/0000-0002-4461-6128>

REFERENCES

- Sellin L, Huber TB, Gerke P, Quack I, Pavenstädt H, Walz G. NEPH1 defines a novel family of podocin interacting proteins. *FASEB J Off Publ Fed Am Soc Exp Biol*. 2003;17:115-117.
- Gerke P, Benzing T, Hohne M, et al. Neuronal expression and interaction with the synaptic protein CASK suggest a role for Neph1 and Neph2 in synaptogenesis. *J Comp Neurol*. 2006;498:466-475.
- Morikawa Y, Komori T, Hisaoka T, Ueno H, Kitamura T, Senba E. Expression of mKirre in the developing sensory pathways: its close apposition to nephrin-expressing cells. *Neuroscience*. 2007;150:880-886.
- Serizawa S, Miyamichi K, Takeuchi H, Yamagishi Y, Suzuki M, Sakano H. A neuronal identity code for the odorant receptor-specific and activity-dependent axon sorting. *Cell*. 2006;127:1057-1069.
- Tamura S, Morikawa Y, Hisaoka T, Ueno H, Kitamura T, Senba E. Expression of mKirre, a mammalian homolog of drosophila kirre, in the developing and adult mouse brain. *Neuroscience*. 2005;133:615-624.
- Völker LA, Petry M, Abdelsabour-Khalaf M, et al. Comparative analysis of Neph gene expression in mouse and chicken development. *Histochem Cell Biol*. 2012;137:355-366.
- Maness PF, Schachner M. Neural recognition molecules of the immunoglobulin superfamily: signaling transducers of axon guidance and neuronal migration. *Nat Neurosci*. 2007;10:19-26.
- Pollerberg GE, Thelen K, Theiss MO, Hochlehnert BC. The role of cell adhesion molecules for navigating axons: density matters. *Mech Dev*. 2013;130:359-372.
- Shen K, Bargmann CI. The immunoglobulin superfamily protein SYG-1 determines the location of specific synapses in *C. elegans*. *Cell*. 2003;112:619-630.
- Prince JEA, Brignall AC, Cutforth T, Shen K, Cloutier J-F. Kirrel3 is required for the coalescence of vomeronasal sensory neuron axons into glomeruli and for male-male aggression. *Dev Camb Engl*. 2013;140:2398-2408.
- Fuchs PA, Glowatzki E, Moser T. The afferent synapse of cochlear hair cells. *Curr Opin Neurobiol*. 2003;13:452-458.
- Martin EA, Muralidhar S, Wang Z, et al. The intellectual disability gene Kirrel3 regulates target-specific mossy fiber synapse development in the hippocampus. *Elife*. 2015;4:e09395.
- Anney RL, Lasky-Su J, Ó'Dúshláine C, et al. Conduct disorder and ADHD: evaluation of conduct problems as a categorical and quantitative trait in the international multicentre ADHD genetics study. *Am J Med Genet B Neuropsychiatr Genet*. 2008;147B:1369-1378.
- Talkowski ME, Rosenfeld JA, Blumenthal I, et al. Sequencing chromosomal abnormalities reveals neurodevelopmental loci that confer risk across diagnostic boundaries. *Cell*. 2012;149:525-537.
- Bhalla K, Luo Y, Buchan T, et al. Alterations in CDH15 and KIRREL3 in patients with mild to severe intellectual disability. *Am J Hum Genet*. 2008;83:703-713.
- Guerin A, Stavropoulos DJ, Diab Y, et al. Interstitial deletion of 11q implicating the KIRREL3 gene in the neurocognitive delay associated with Jacobsen syndrome. *Am J Med Genet A*. 2012;158A:2551-2556.
- So J, Stockley T, Stavropoulos DJ. Periventricular nodular heterotopia and transverse limb reduction defect in a woman with interstitial 11q24 deletion in the Jacobsen syndrome region. *Am J Med Genet A*. 2014;164:511-515.
- Grahammer F, Wigge C, Schell C, et al. A flexible, multilayered protein scaffold maintains the slit in between glomerular podocytes. *JCI Insight*. 2016 Jun 16;1(9). pii: e86177.

19. Schwenk F, Baron U, Rajewsky K. A cre-transgenic mouse strain for the ubiquitous deletion of loxP-flanked gene segments including deletion in germ cells. *Nucleic Acids Res.* 1995;23:5080-5081.
20. Wagener RJ, Dávid C, Zhao S, Haas CA, Staiger JF. The somatosensory cortex of reeler mutant mice shows absent layering but intact formation and behavioral activation of columnar somatotopic maps. *J Neurosci Off J Soc Neurosci.* 2010;30:15700-15709.
21. Schurek E-M, Völker LA, Tax J, et al. A disease-causing mutation illuminates the protein membrane topology of the kidney-expressed prohibitin homology (PHB) domain protein podocin. *J Biol Chem.* 2014;289:11262-11271.
22. Crawley J. *What's Wrong with my Mouse?: Behavioral Phenotyping of Transgenic and Knockout Mice.* Hoboken, NJ: Wiley-Interscience; 2007.
23. Crawley JN, Paylor R. A proposed test battery and constellations of specific behavioral paradigms to investigate the behavioral phenotypes of transgenic and knockout mice. *Horm Behav.* 1997;31:197-211.
24. Kinney JW, Starosta G, Holmes A, et al. Deficits in trace cued fear conditioning in galanin-treated rats and galanin-overexpressing transgenic mice. *Learn Mem Cold Spring Harb N.* 2002;9:178-190.
25. Paylor R, Nguyen M, Crawley JN, Patrick J, Beaudet A, Orr-Urtreger A. Alpha7 nicotinic receptor subunits are not necessary for hippocampal-dependent learning or sensorimotor gating: a behavioral characterization of Acra7-deficient mice. *Learn Mem Cold Spring Harb N.* 1998;5:302-316.
26. Albayram Ö, Passlick S, Bilkei-Gorzo A, Zimmer A, Steinhäuser C. Physiological impact of CB1 receptor expression by hippocampal GABAergic interneurons. *Pflüg Arch—Eur J Physiol.* 2016;468:727-737.
27. Willott JF, Erway LC, Archer JR, Harrison DE. Genetics of age-related hearing loss in mice. II. Strain differences and effects of caloric restriction on cochlear pathology and evoked response thresholds. *Hear Res.* 1995;88:143-155.
28. Komori T, Gyobu H, Ueno H, Kitamura T, Senba E, Morikawa Y. Expression of kin of irregular chiasm-like 3/mKirre in proprioceptive neurons of the dorsal root ganglia and its interaction with nephrin in muscle spindles. *J Comp Neurol.* 2008;511:92-108.
29. Luján R, Albasanz JL, Shigemoto R, Juiz JM. Preferential localization of the hyperpolarization-activated cyclic nucleotide-gated cation channel subunit HCN1 in basket cell terminals of the rat cerebellum. *Eur J Neurosci.* 2005;21:2073-2082.
30. Buttermore ED, Piochon C, Wallace ML, Philpot BD, Hansel C, Bhat MA. Pinceau Organization in the Cerebellum Requires Distinct Functions of Neurofascin in Purkinje and basket neurons during postnatal development. *J Neurosci.* 2012;32:4724-4742.
31. Laube G, Röper J, Pitt JC, et al. Ultrastructural localization of shaker-related potassium channel subunits and synapse-associated protein 90 to septate-like junctions in rat cerebellar Pinceaux. *Brain Res Mol Brain Res.* 1996;42:51-61.
32. Liu YF, Sowell SM, Luo Y, et al. Autism and intellectual disability-associated KIRREL3 interacts with neuronal proteins MAP1B and MYO16 with potential roles in neurodevelopment. *PLoS One.* 2015;10:e0123106.
33. Choi S-Y, Han K, Cutforth T, et al. Mice lacking the synaptic adhesion molecule Neph2/Kirrel3 display moderate hyperactivity and defective novel object preference. *Front Cell Neurosci.* 2015;9:283.
34. Hisaoka T, Komori T, Kitamura T, Morikawa Y. Abnormal behaviours relevant to neurodevelopmental disorders in Kirrel3-knockout mice. *Sci Rep.* 2018;8:1408.
35. Brignall AC, Raja R, Phen A, Prince JEA, Dumontier E, Cloutier J-F. Loss of Kirrel family members alters glomerular structure and synapse numbers in the accessory olfactory bulb. *Brain Struct Funct.* 2018 Jan;223(1):307-319.
36. Martin EA, Woodruff D, Rawson RL, Williams ME. Examining hippocampal mossy fiber synapses by 3D electron microscopy in wildtype and Kirrel3 knockout mice. *ENeuro.* 2017;4:ENEURO.0088-ENEU17.2017.
37. Roh JD, Choi S-Y, Cho YS, et al. Increased excitatory synaptic transmission of dentate granule neurons in mice lacking PSD-95-interacting adhesion molecule Neph2/Kirrel3 during the early postnatal period. *Front Mol Neurosci.* 2017;10:81.
38. Ding M, Chao D, Wang G, Shen K. Spatial regulation of an E3 ubiquitin ligase directs selective synapse elimination. *Science.* 2007;317:947-951.
39. Nishida, K., Nakayama, K., Yoshimura, S., and Murakami, F. (2011). Role of Neph2 in pontine nuclei formation in the developing hind-brain. *Mol Cell Neurosci.* In Press, Accepted Manuscript.
40. Paul A, Huang ZJ. Developmental coordination of gene expression between synaptic partners during GABAergic circuit assembly in cerebellar cortex. *Front Neural Circuits.* 2012;6:37.
41. Ango F, di Cristo G, Higashiyama H, Bennett V, Wu P, Huang ZJ. Ankyrin-based subcellular gradient of Neurofascin, an immunoglobulin family protein, directs GABAergic innervation at Purkinje axon initial segment. *Cell.* 2004;119:257-272.
42. Ahn AH, Dziennis S, Hawkes R, Herrup K. The cloning of zebrin II reveals its identity with aldolase C. *Development.* 1994;120:2081-2090.
43. Sillitoe RV, Stephen D, Lao Z, Joyner AL. Engrailed homeobox genes determine the organization of Purkinje cell sagittal stripe gene expression in the adult cerebellum. *J Neurosci Off J Soc Neurosci.* 2008;28:12150-12162.

SUPPORTING INFORMATION

Additional supporting information may be found online in the Supporting Information section at the end of the article.

How to cite this article: Völker LA, Maar BA, Pulido Guevara BA, et al. Neph2/Kirrel3 regulates sensory input, motor coordination, and home-cage activity in rodents. *Genes, Brain and Behavior.* 2018;17:e12516. <https://doi.org/10.1111/gbb.12516>